Journal of Membrane Science 611 (2020) 118367

Contents lists available at ScienceDirect

Journal of Membrane Science

journal homepage: http://www.elsevier.com/locate/memsci

Fabrication of pervaporation desalination membranes with excellent chemical resistance for chemical washing

Pengbo Zhao, Yunlong Xue, Rui Zhang, Bing Cao **, Pei Li *

College of Materials Science and Engineering, Beijing University of Chemical Technology, Beijing, 100029, China

ARTICLE INFO

Keywords:
Pervaporation desalination
Composite membrane
Membrane washing
Chemical resistance

ABSTRACT

Pervaporation membranes have exhibited great potential for desalinating brine solutions. However, the flux recovery after membrane washing and the membrane's resistance to chemical cleaning reagents were barely studied. Our group has reported excellent desalination properties of PVA based pervaporation membranes. Nevertheless, the membranes were damaged during chemical cleaning due to the poor chlorine resistance of PVA. In this study, the more active 1, 2-diol units of PVA were removed by sodium periodate treatment. And then, the modified PVA was crosslinked by FS-3100, a fluorocarbon based crosslinker, to improve its hydrostability and chlorine resistance. The FS-3100 crosslinked composite (PVA-FS/PVDF) showed a water flux of 34 ± 1 kg m^{-2} h^{-1} with a NaCl rejection of 99.93% when desalinated a 35000 ppm NaCl solution at 70 °C. Salt rejections were maintained after soaking in 2000 ppm NaClO, acid (pH = 2), and alkali (pH = 12) solutions for 168, 180, and 180 h, respectively. A long term desalination experiment was carried out using Tween 20 and HA as foulants. The water fluxes could be recovered to 100% after chemical washing without losing salt rejections, indicating an excellent long term operation stability of the FS-3100 crosslinked PV membranes.

1. Introduction

Water scarcity and environmental pollution are global issues [1], which can be solved by water separation membrane technologies [2,3]. Today, reverse osmosis (RO) dominates the market of seawater desalination because of the high water quality and low energy consumption (3–4 kw h·ton^{-1}). It, however, generates large amount of concentrated brine solution that endangers environment [4]. Recently, pervaporation (PV) membranes have been developed rapidly for desalination because of their potential for treating concentrated salt solution [5]. Although PV desalination needs a lot of heat to evaporate water, the energy consumption can be reduced to 1.5–5.9 kw h·ton^{-1} upon using renewable or waste heat [6]. Moreover, unlike membrane distillation (MD) that faces troublesome fouling issues, the hydrophilic nature of the dense selective layer of PV membranes enables excellent fouling resistance similar to antifouling RO/UF membranes coated with a hydrophilic layer [7–10]. Nevertheless, PV desalination membranes can still be fouled and show gradually deteriorated desalination properties [11].

Pollutants in surface water or seawater are usually natural organic matters (NOMs), while effluent organic matters (EOM) are typical foulants in wastewater [12]. Once a membrane is fouled, flux can be recovered by chemical cleaning using acid, alkali, enzyme, redox, complexing agent, surfactant, disinfectant et al. [13–15]. Among these chemical compounds, sodium hypochlorite (NaClO) is very effective for removing NOMs and EOMs [16]. However, it requires membrane materials having excellent chlorine resistance [17].

Polyvinyl alcohol (PVA) is widely used in PV membranes due to its good film forming property and hydrophilicity [6,18]. It is reported that PVA is the only one to be consolidated at industrial level [19]. For instance, DeltaMem currently manufactures and commercializes crosslinked PVA membranes for PV applications [20]. It is reported that PVA has good tolerance to acid, and alkali [21–24]. However, PVA is not stable in NaClO solution. As shown in Scheme 1a, PVA has 1, 2-diol and 1, 3-diol units. The presence of 1, 2-diol restricts densely packing of PVA chains. The oxidants, ClO^- or HClO, will diffuse into the loosely packed 1, 2-diol segments easier than the densely packed 1, 3-diol regions. As a result, 1, 2-diol is more vulnerable in NaClO solution and will be oxidized to C═O [25], which will be further oxidized to COOH and lead to chain cleavage between C═O and α-C. Some researchers improved the chlorine resistance of PVA by removing 1, 2-diols [26]. This was

* Corresponding author.
** Corresponding author.
E-mail addresses: bcao@mail.buct.edu.cn (B. Cao), lipei@mail.buct.edu.cn (P. Li).

https://doi.org/10.1016/j.memsci.2020.118367
Received 10 April 2020; Received in revised form 18 May 2020; Accepted 5 June 2020
Available online 10 June 2020

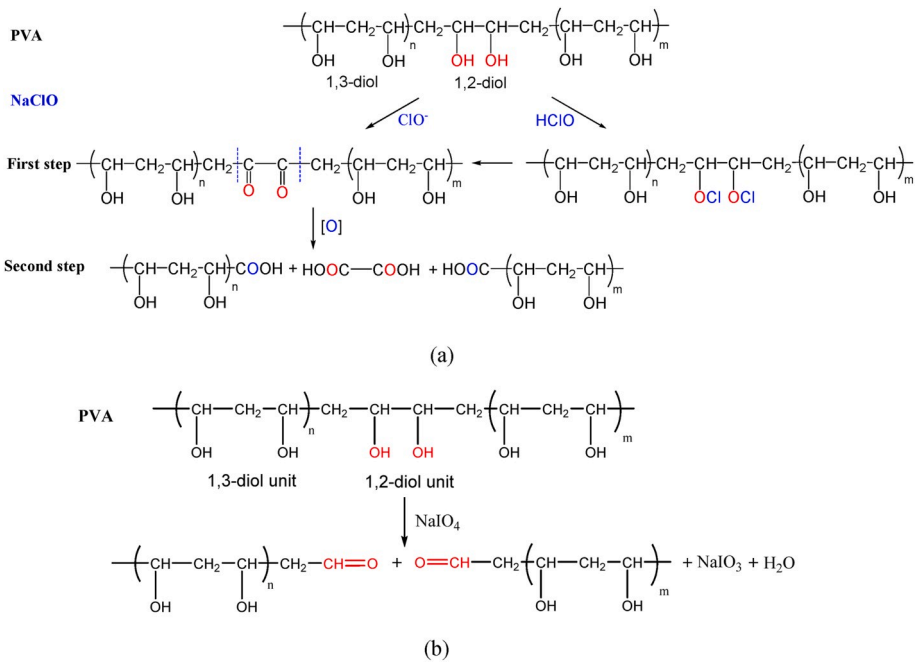

Scheme 1. The oxidation mechanisms of PVA in aqueous solutions of NaClO (a) and $NaIO_4$(b).

done by oxidizing 1, 2-diols using sodium periodate ($NaIO_4$) as shown in Scheme 1b [27]. $NaIO_4$ broke the carbon-carbon bond of the 1, 2-diol unit and formed aldehyde groups. The remaining 1, 3-diols led to higher syndiotacticity and crystallinity of PVA and resulted in better chlorine resistance [28].

Crosslinking is a well-known methodology to enhance chlorine resistance of polymeric membranes [29,30]. For PVA based PV membranes, crosslinking is mandatory to prevent dissolution of PVA in aqueous solution. Since fluorocarbons typically show excellent stability in harsh environments, we expect that using fluorocarbon containing chemicals to crosslink PVA shall effectively improve the chlorine resistance as reported in literatures [31–34].

Here in this work, the chlorine resistance of PVA was improved via a two-prong strategy, i.e. the PVA was first modified by removing the 1, 2-diols, and then crosslinked by FS-3100, a substitute of surfactant FSO-100 with a molecular formula of $F(CF_2CF_2)_nCH_2CH_2O\ (CH_2CH_2O)_mH$ (n = 0–25, m = 1–9). The crosslinked PVA was used to prepare composite membranes. Stabilities of the membranes were evaluated in acid, alkali, and chlorine solutions. At last, a membrane washing protocol was carried out to regenerate water flux during long term PV desalination experiments. To our best knowledge, this is the first study focusing on improving chlorine tolerance of PV desalination membranes for chemical washing.

2. Experimental

2.1. Materials

The PVA powder (M_w 105,000 g mol^{-1}, hydrolysis degree 98%) was purchased from Merck Schuchart Chemical Reagent Co., Ltd (China). Deionized (DI) water was produced using a lab equipped Millipore ultrapure water system. Humic acid (HA) was provided by Kmart Chemical Technology Co., Ltd (Tianjin, China). Polyoxyethylene sorbitan monolaurate (Tween 20) was obtained from Baibei Biological Technology Co., Ltd (Tianjin, China). The fluorocarbon surfactant (FS-3100) was provided by DuPont (Shanghai, China). PET non-woven fabric was got from Shanghai Poly Technology Co., Ltd.

2.2. PVA modification and preparation of the PVA-FS membranes

3 g of PVA was dissolved in 97 mL of DI water. 1.5 g of sodium periodate was added to the PVA solution which was then stirred at room temperature for 10 min. An excess amount of acetone was poured into the PVA solution. Consequently, PVA polymer gradually precipitated from the solution in 12 h. The turbid solution was filtered to collect the PVA powder which was rinsed with DI water and dried in vacuum before use.

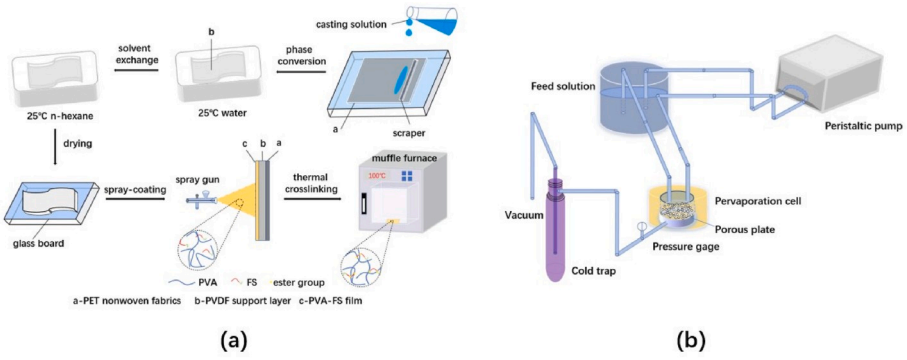

Fig. 1. Schematic diagrams of (a) PV composite membrane preparation and (b) pervaporation device.

The PVDF ultra-filtration membrane, used as the support of PV composite membrane, was prepared by knife-casting a PVDF polymer dope on to a polyester nonwoven fabric. The composite was immersed in DI water to induce non-solvent induced phase inversion process [35]. After the PVDF layer solidified, water in the composite was exchanged by methanol followed by n-hexane. Finally, the PVDF membrane was dried in air before use.

To fabricate the PV composite membranes, 3 wt% PVA solution was mixed with FS-3100 at varied amounts. pH value of the mixed solution was adjusted to 1 by adding sulfuric acid as crosslinking catalyst. The molar ratio of carboxylic acid groups of FS-3100 to hydroxyl groups in PVA was controlled as: n(COOH):n(OH) = 1:100, 1:80, 1:60, 1:40, and 1:20, respectively. The PVA/FS-3100 mixed solution was spray-coated on to the PVDF membrane using an air-brush. Details of the spray-coating process could be found elsewhere [36]. The PVA layer was dried in air and crosslinked in a muffle furnace at 100 °C for 15–20 min (Fig. 1a). Using a similar protocol, the 4-sulfophthanlic acid (SPTA) [5] and poly(acrylic acid-co-2-acrylamido-2-methyl propane sulfonic acid (P(AA-AMPS)) [6] crosslinked PVA/PVDF composite membranes were prepared and used as controlled samples. The resistances to acid, base, and chlorine solutions of the PVA based composite membranes crosslinked by SPTA, P(AA-AMPS), and FS-3100 were compared.

2.3. Characterization

Fourier transform infrared spectroscopy (ATR-FTIR, Nicolet 560) and nuclear magnetic resonance proton spectroscopy (NMR, AVANCE III 400, Bruker BioSpin GmbH, Germany) were used to verify the complete removal of 1, 2-diols groups in PVA after modifications. The decrement in PVA molecular weight over modification time was measured by gel permeation chromatography (GPC, LC15RI). An iodometry (GB/T 19106-2003) was used to determine the effective chlorine concentration in NaClO solutions. The area ratios of FTIR peaks at 1145 cm^{-1} to 1095 cm^{-1} (D1145/D1095) and 916 cm^{-1} to 849 cm^{-1} (D916/D849) were calculated to determine the crystallinity and syndiotacticity of PVA. The syndiotacticity S (%) of PVA was defined as the percentage of the hydroxyl groups which were alternately distributed on the PVA backbone. S% of PVA was calculated by Eq. (1) [37]:

$$S = 71.1 \times \left(\frac{D_{916}}{D_{849}}\right)^{0.327} \quad (1)$$

To determine the values of 'n' and 'm' of $F(CF_2CF_2)_nCH_2CH_2O(CH_2CH_2O)_mH$, FS-3100 were characterized by ATR-FTIR, ^{13}C NMR, ^{1}H NMR and ^{19}F NMR. Surface of the PV composite membranes were monitored by ATR-FTIR to verify the chemical structure of the FS-3100 crosslinked PVA (PVA-FS). The PVA-FS layer thicknesses were measured using a field emission scanning electron microscope (SEM, Nova Tecnai G2 F20, FEI, USA). The samples were fractured in liquid nitrogen to get a smooth cross-sectional morphology. X-ray diffractometry (XRD) spectra were observed using an X-ray diffractometer (D8 Advance, Bruker BioSpin, Germany) with a Cu Kα radiation wavelength of 1.54 Å.

2.4. Pervaporation tests

Fig. 1b shows the apparatus for pervaporation desalination tests. A water solution containing 35,000 ppm NaCl at 70 °C was circulated at membrane feed side using a peristaltic pump (BT600-2J, Langer, USA). To avoid the polarization effect, the peristaltic pump was operated at 400 r·min^{-1} corresponding to a flow rate of 0.35 m s^{-1}. At this flow speed, the Reynolds's number was 4700, indicating a turbulent flow status. It was observed that a further increase in rotation rate did not result in any increment in water flux. It meant that the polarization effects had been controlled at a minimal level. Membrane permeate side was vacuumed at 100 Pa to draw over water vapor. Water flux (J_A) was determined by Eq. (2):

$$J_A = \frac{m}{S \times T} \quad (2)$$

where m (kg) was the water collected in a cold trap; s was the effective membrane area (m^2); and t was the experiment time (h). Salt rejection (R) was calculated by Eq. (3):

$$R = \frac{C_f - C_p}{C_p} \times 100\% \quad (3)$$

where C_f, C_p were the salt concentrations of the feed and permeate solutions. Because of the non-volatility of salt, C_p was determined in an indirect way. After each PV test, the permeate side of membrane was washed with DI water. A conductivity meter (Con 110, Thermo Fish OAKTON, Singapore) was used to measure the NaCl concentration of the solution. Water permeance ($\overline{P_w}$) was determined by Eq. (4):

$$\overline{P_w} = \frac{J}{\Delta p} \quad (4)$$

where J was the water vapor flux (cm^3(stp)/(cm^2s)); Δp was the trans-membrane pressure difference of the water vapor (cmHg); water permeance was reported in GPU (1 GPU = 1 × 10^{-6} cm^3(stp)/(cm^2·s·cmHg)). Water permeability was calculated using Eq. (5):

$$P_w = \overline{P_w} \times L \quad (5)$$

where L was the dense layer thickness in an unit of cm and P_w was the water permeability in an unit of barrer (1 barrer = 1 × 10^{-10} cm^3(stp)·cm/(cm^2·s·cmHg)).

2.5. Determination of crosslinking density

Self-standing PVA-FS thick films were prepared to measure the crosslinking density. By casting a PVA/FS solution on a PTFE board, a film with thickness of 50 ± 10 μm was formed by evaporating water at room temperature for 24 h and then crosslinked at 100 °C in a muffle furnace for 20 min. The ratio of n(COOH): n(OH) in the PVA/FS-3100 solution was controlled at 1:100, 1:80, 1:60, 1:40, and 1:20, respectively. The net weight was recorded as m_0 (mg). The fully dried film was soaked in 25 °C deionized water for at least 48 h to ensure that the swelled films had reached to sorption equilibrium. The wet films were wiped carefully with tissue paper to remove water attached on the film surface. To minimize solvent evaporation, each weighing process was carried out within 30 s. The saturated mass of swelled PVA-FS film was recorded as m_1 (mg). Crosslinking density ρ_c (mol·m^{-3}) was determined by Eq. (6):

$$\rho_c = \frac{1}{M_c} \quad (6)$$

where Mc (g·mol^{-1}) was the average molecular weight of the molecular chain between the two crosslinking points. M_c (g·mol^{-1}) was determined by Equation (7) [38]:

$$\ln \varphi_1 + \varphi_2 + \chi\varphi_2^2 + \frac{\rho V_m}{M_c} \times \varphi_2^{\frac{1}{3}} = 0 \quad (7)$$

where ϕ_1 was the volume fraction of the solvent in the gel. ϕ_2 was the volume fraction of the polymer in the gel. ϕ_1 and ϕ_2 were determined by swelling experiments. ρ (g·cm^{-3}) was the density of the polymer. V_m (mol·cm^{-3}) was the molar volume of the solvent. χ was the Flory-Huggins interaction parameter between solvent and polymer. The Flory-Rehner theory was used to describe the polymer swelling behavior, and χ was calculated using Equation (8) [39]. ρ could be obtained with a solid-liquid multifunctional density tester (DE-120X) according to Equation (9):

Table 1
Molecular weights, peak area ratios and syndiotacticity of PVA over oxidation times.

Oxidation time (min)	M_n	M_w	$\frac{D_{916}}{D_{849}}$	S (%)	$\frac{D_{1145}}{D_{1095}}$
0	57128 ± 40	127455 ± 78	0.58 ± 0.09	58.82 ± 1.28	0.43 ± 0.06
10	8620 ± 22	11715 ± 32	0.73 ± 0.11	64.15 ± 1.54	0.68 ± 0.09
30	8346 ± 18	10906 ± 28	0.76 ± 0.08	65.00 ± 1.15	0.69 ± 0.07

$$\chi = \frac{\ln(\varphi_i) - (1-\varphi_i)}{(1-\varphi_i)^2} \tag{8}$$

$$\rho = \frac{A}{A-B} + (\rho_0 + \rho_L) + \rho_L \tag{9}$$

where ϕ_i was the volume fraction of the polymer in the gel. ρ_0 was density of auxiliary liquid (DI water or absolute ethanol). ρ_L was the air density (0.0012 g cm^{-3}). A was the sample's weight in air, while B was its weight in auxiliary liquid.

2.6. Evaluating the chlorine resistance

Chlorine resistance was determined by soaking a piece of PV membrane, which was crosslinked by SPTA, P(AA-AMPS), or FS-3100, into 2000 ppm sodium hypochlorite (NaClO) solution for 168 h the longest. After every 12 h, the membrane was taken out and tested for PV desalination properties. The possible changes in chemical structure, hydrophilicity, and surface charge of the PVA-FS layers over the soaking time were monitored by ATR-FTIR, water contact angle (JC2000C, Powereach, Shanghai, China), and zeta potential (DelsaNano C, Beckman Coulter Diagnostics, China).

2.7. Acid and alkali tolerance

Acid resistances were determined by monitoring the water flux and salt rejections of the PV membranes after soaked in acid solutions of pH of 1 or 2, respectively. The PV desalination tests were carried out after every 12 h soaking time and continued until an obvious declination in salt rejection was observed. Using a similar method, alkali tolerances were evaluated by soaking the membranes in base solutions with pH of 13 or 14, respectively, and measured the desalination properties.

2.8. Membrane fouling and washing experiments

PV tests were performed at a feed temperature of 70 °C. Pure water flux was measured first and labeled as J_{w1}. Then, a Tween20 or HA (1.0 g L^{-1}) aqueous solution was used as feed and the PV experiment was running for 10 h. Membrane surface was washed by a NaOH solution (pH = 12) for 30 min. Pure water flux was measured again and labeled as J_{w2}. The PV test was further running for 5 h using a feed solution containing 1.0 g L^{-1} Tween20 or HA. Membrane surface was washed using a NaClO solution (200 ppm) for 30 min. Pure water flux was measured and recorded as J_{w3}. Flux recovery ratio (*FRR*) were calculated by equations (10) and (11):

$$FRR_{NaOH} = \frac{J_{W_2}}{J_{W_1}} \times 100\% \tag{10}$$

$$FRR_{NaClO} = \frac{J_{W_3}}{J_{W_1}} \times 100\% \tag{11}$$

3. Results and discussion

3.1. Material characterizations

$NaIO_4$ could oxidize the 1, 2-diol units of PVA and break the molecular chains. As listed in Table 1, molecular weights of PVA rapidly decreased after soaking in $NaIO_4$ solution for 10 min. As the oxidation time increased further, it only led to a slightly decrement in molecular weight, indicating a completely removal of the 1,2-diol units. This conclusion was verified by the FTIR spectra in Fig. 2a where the main decrement in peak area at 3275 cm^{-1}, representing the –OH groups, took place after 10 min of $NaIO_4$ treatment. The peak at 1145 cm^{-1} was the symmetrical stretching vibration peak of O–C–C groups, while the peak at 1095 cm^{-1} was the anti-symmetric stretching vibration peak of O–C–C [40]. As polymer crystallinity increased, intensity of the peak at 1145 cm^{-1} and the quotient of peak areas of 1145 to 1095 cm^{-1} should increase [37]. As listed in Table 1, D_{1145}/D_{1095} increases from 0.43 ± 0.06 to 0.68 ± 0.09 after 10 min of NaClO treatment, and slightly increases to 0.69 ± 0.07 after another 20 min treatment. This again indicated that the 1, 2-diol groups were mostly decomposed in the first 10 min. The syndiotacticity S% of PVA could be determined from the peaks at 916 cm^{-1} and 849 cm^{-1}, respectively, using Equation (1). According to Table 1, the increase in S% is mainly happened in the first 10 min of oxidation treatment.

Chlorine tolerances of the PVA polymer before and after $NaIO_4$ treatment were evaluated by soaking the PVA samples in chlorine solution and monitoring the changes in ClO^- concentration over time. The consumption of ClO^- could be calculated by minus the real time ClO^- concentration from the initial ClO^- concentration. As shown in Fig. 2b, the effective chlorine consumption rate of the $NaIO_4$ treated PVA was much lower than that of the virgin PVA, indicating its chlorine resistance was improved. However, the $NaIO_4$ treated PVA still consumed considerably amount of chlorine, which meant that the chlorine resistance needed further improvement.

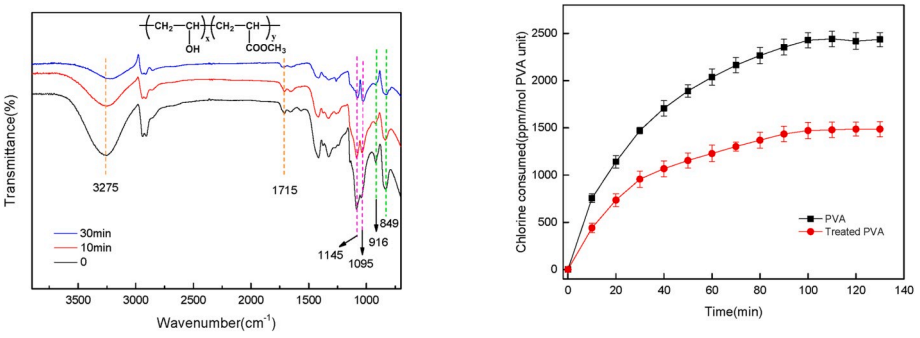

(a) (b)

Fig. 2. (a) FTIR spectra of PVA at different oxidation times, (b) plot of chlorine consumption versus period of reaction.

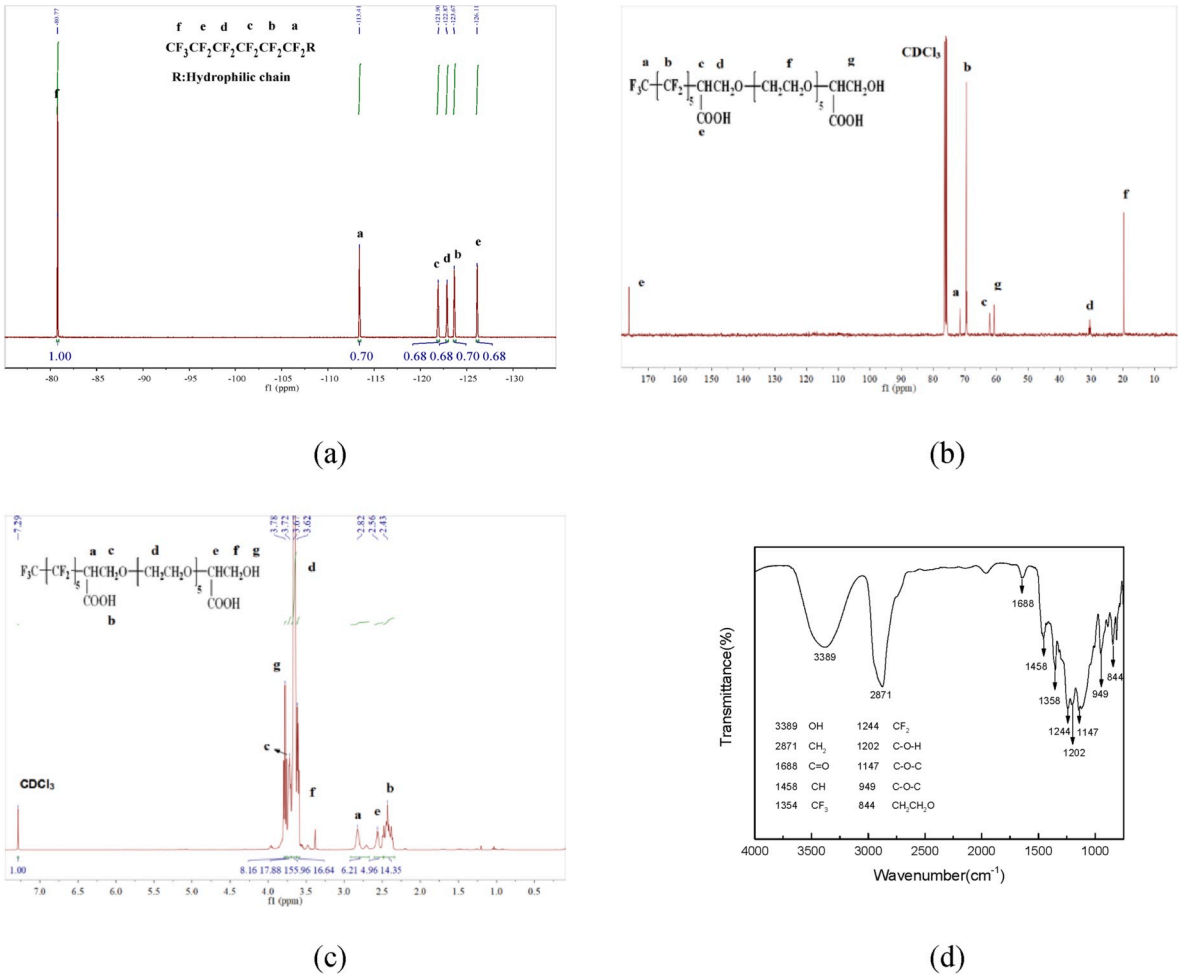

Fig. 3. (a) ^{19}F NMR spectra, (b)^{13}C NMR spectra, (c) ^{1}H NMR spectra and (d)FTIR spectra of FS-3100.

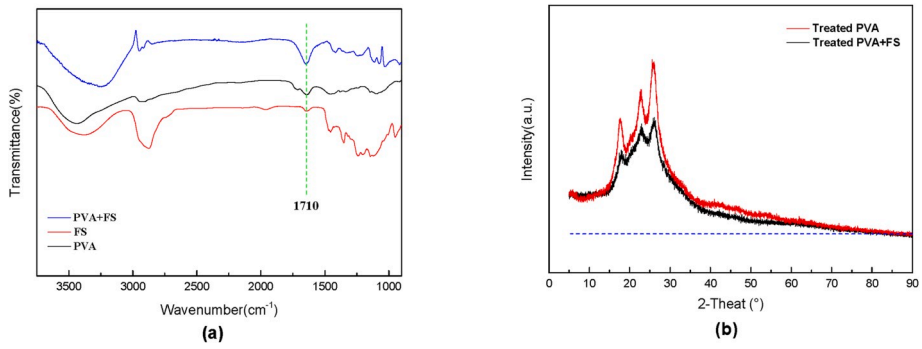

Fig. 4. (a) FTIR spectra of PVA/FS/PVA + FS, (b) XRD spectra of PVA and PVA-FS membrane.

Chemical structure of FS-3100 was determined by FTIR and NMR as shown in Fig. 3. The peaks at 1147 cm^{-1}, 949 cm^{-1}, and 844 cm^{-1} represented the stretching vibration of the ether bond, the C–O–C in-plane deformation vibration, and the CH_2CH_2O in-plane deformation vibration, respectively. The peaks in the F^{19}-NMR spectra represented the six fluorine atoms located in the FS-3100 molecules with an integral ratio of 3:2:2:2:2:2, which indicated the structure of fluorocarbon segment $CF_3[CF_2]_5$. The C^{13}-NMR spectra show 7 peaks relative to 7 locations of carbon atoms in the FS-3100 molecule. The H NMR spectra show 7 proton peaks with an integration area ratio of a: b: c: d: e: f: g = 6: 14: 18: 156: 5: 17: 8 ≈ 1: 2: 2: 20: 1: 2: 1, which agreed well with the hydrogen ratio of the structure shown in the plot. Therefore, the molecular formula of FS-3100 should be $CF_3(CF_2CF_2)_5CHCOOHCH_2O(CH_2CH_2O)_5CHCOOHCH_2OH$.

3.2. Characterization of PV composite membranes

The crosslink structure of PVA-FS was verified by FTIR as shown in Fig. 4a. The peak intensity at 1710 cm^{-1} was much higher than the pristine PVA and FS-3100, indicating that the ester groups formed after crosslinking. As shown in the XRD spectra in Fig. 4b, the sharp peaks relative to the crystalline regions of PVA became weaker after crosslink. This was because crosslink limited chain mobility and prevented the formation of crystalline structure. The SEM images (Fig. 5) showed that

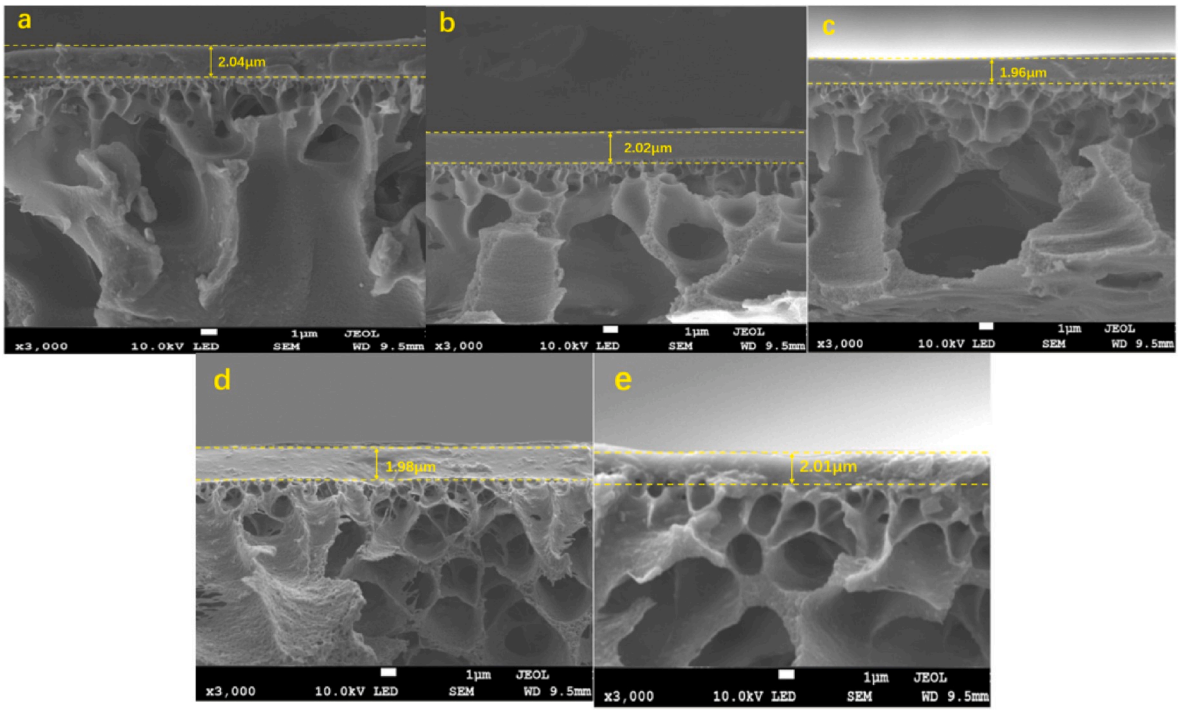

Fig. 5. SEM images of the cross section morphologies of (a) 1:100, (b) 1:80, (c) 1:60, (d) 1:40, (e) 1:20-PVA-FS/PVDF membranes.

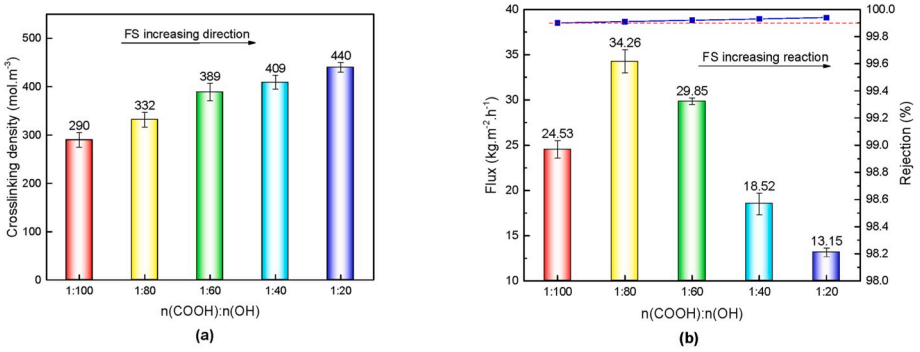

Fig. 6. The relations between the FS-3100 concentrations with (a) the crosslinking density of PVA-FS layers, (b) the pervaporation desalination properties of all PVA-FS/PVDF composite membranes at 70 °C.

all PVA-FS/PVDF composite membranes had a similar PVA-FS layer thickness of 2 μm.

3.3. Crosslinking density and pervaporation desalination properties

As shown in Fig. 6a, with the increase in the crosslinker's concentration, the crosslinking densities gradually increase. Fig. 6b shows that all composite membranes have salt rejections over 99.9%, demonstrating that their skin layers were defect-free. However, water flux increased first and then decreased with the FS-3100 content. This phenomenon could be explained by the overall impact of crosslinking on the decrement in both PVA crystallinity and chain mobility. Low

Table 2
Comparison of desalination permeances of different PV membranes using the 3.5 wt% NaCl solutions as feed.

Membrane ID	Dense layer thickness (μm)	Water flux ($kg \cdot m^{-2} \cdot h^{-1}$)	Salt rejection (%)	Feed temperature (°C)	Water permeance ($\times 10^4$ GPU)	Water permeability ($\times 10^4$ Barrer)
S-PVA/PAN [45]	2.5	9.5	99.7	30	14.8	38.2
S-PVA/PTFE [36]	2.6	43.4	99.9	75	17.7	46.0
S-PVA/PVDF/PTFE [46]	2.3	83.4	99.9	70	17.1	39.4
MXene/PAN [47]	0.06	85.4	99.5	65	12.0	0.72
PVA-PMDA/PAN [48]	2.0	32.26	99.98	70	10.5	20.8
PVA-FS/PVDF	2.0	34.3	99.93	70	11.0	21.9

1 GPU = 1×10^{-6} cm^3(stp)/(cm^2·s·cmHg); 1 Barrer = 1×10^{-10} cm^3(stp)·cm/(cm^2·s·cmHg). PSF: polysulfone; PVDF: polyvinylidene fluoride; PAN: polyacrylonitrile; PMDA: pyromellitic dianhydride.

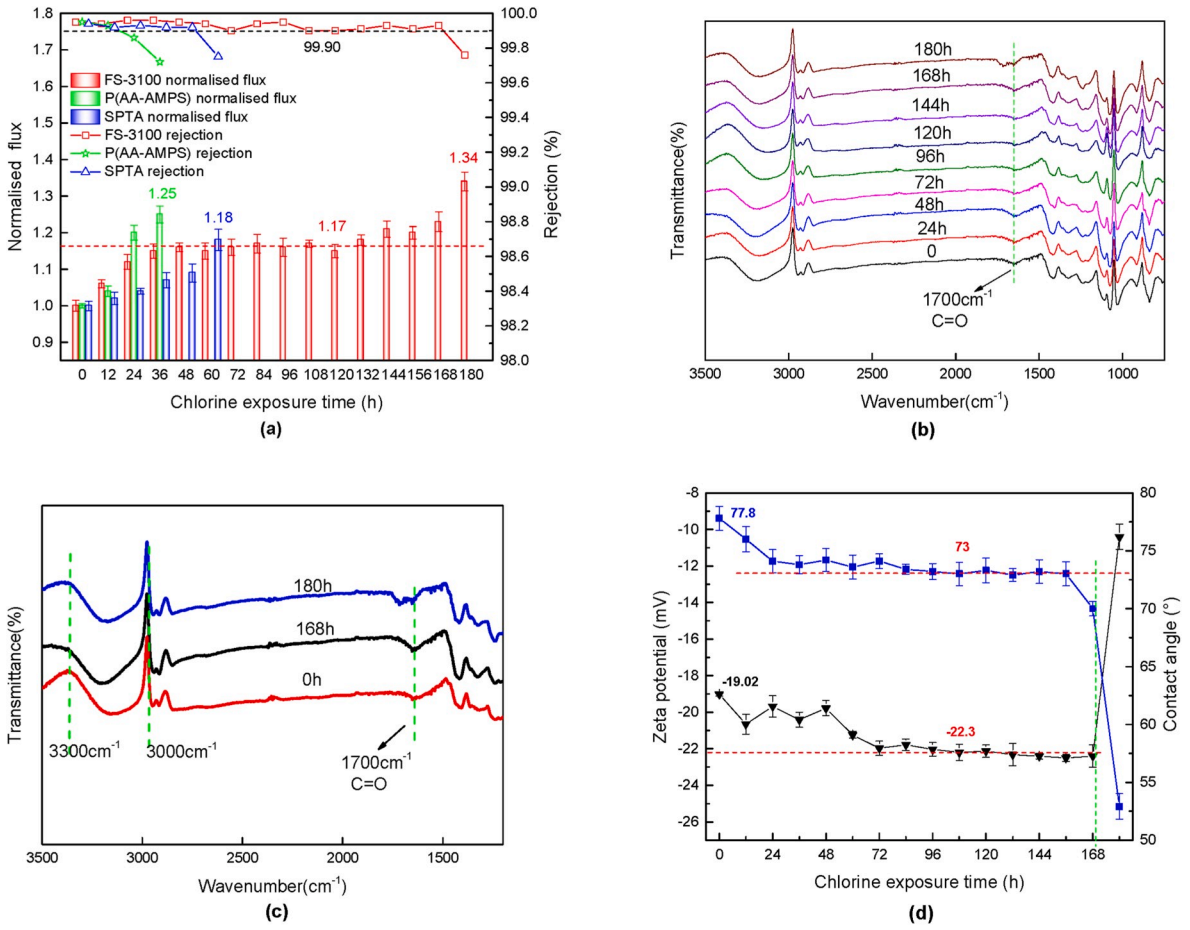

Fig. 7. Chlorine resistance of membranes in 2000 ppm NaClO (a) respectively using FS, SPTA and P(AA-AMPS) as crosslinker, (b) and (c) FTIR spectra of membranes immersed in 2000 ppm NaClO at different times, (d) zeta potential and contact angle of membranes immersed in 2000 ppm NaClO at different times.

polymer crystallinity favored the diffusion of water, while high crosslinking degree restricted polymer chain rotation and limited water transport. At the relative low crosslinking degree, the decrease in PVA crystallinity overplayed the effect of reducing chain mobility. Therefore, the membrane water flux increased. At higher crosslinking degrees, the rigid PVA network governed the water transport property. Thus, water flux decreased. In addition, the hydrophobic nature of FS-3100 led to the decreased hydrophilicity of the PVA-FS polymer, which in turn caused the membrane water flux decrease at higher FS-3100 concentrations. The optimized composition of the PVA-FS crosslinking system was obtained with n(COOH): n(OH) = 1:80 with the maximum water flux of 34.3 ± 1.3 kg m^{-2} h^{-1} and salt rejection of 99.93%.

Trade-off relations are frequently reported by membrane scientists. However, for PV desalination and MD desalination membranes, salt rejections are found independent to flux and often close to 100%. This is because most salts are non-volatile. Therefore, to assess desalination properties among PV desalination membranes, it is rational to compare their water permeance or permeability [41]. Table 2 lists desalination properties of some representative PV desalination membranes. It can be seen that sulfonated crosslinked PVA based membranes exhibit much higher intrinsic water transport properties including permeance and permeability. These results match the observation that PV membrane with polar group such GO absorbs more water and demonstrates higher water flux [42]. On the other hand, the PVA membranes crosslinked by PMDA and FS-3100, where the crosslinkers do not contain polar groups, show 50% lower water permeability. Clearly, if a material having low permeability, high membrane flux can also be achieved by reducing selective layer thickness. The MXene/PAN composite had a dense layer thickness of 60 nm and showed a very high water flux of 85.4 kg m^{-2} h^{-1} [47]. However, the purpose of this study is to improve the chlorine resistance of the PV membranes. A thinner polymer dense layer may increase water flux but at a risk of weakening chlorine tolerance. Therefore, we maintain the thickness of PVA-FS layer at 2 μm. Note that, water flux of this membrane is still competitive to seawater RO membranes (32–40 kg m^{-2} h^{-1}) [43,44].

3.4. Chlorine resistance

Chlorine resistance of the PVA-FS(1:80)/PVDF composite was determined and compared with the PVA/PVDF membranes crosslinked by SPTA and P(AA-AMPS), as shown in Fig. 7a. If defined the onset decrements in salt rejections as the evidence of the damage to the crosslinked PVA layer by chlorine, the durability in 200 ppm chlorine solution of FS-3100, SPTA, and P(AA-AMPS) crosslinked PVA membranes were 168 h, 48 h, and 24 h, respectively. Therefore, the FS-3100 crosslinked PVA exhibited much better chlorine resistance. Fig. 7b and c show that the shapes and intensities of peaks representing C═O of the ester group in PVA-FS at 1700 cm^{-1} were almost unchanged within 168 h soaking time, but became broad and weak after 180 h. The newly formed peak at 1720 cm^{-1} indicated that some OH groups in PVA were oxidized to –COOH groups by chlorine. Meanwhile, intensity of the broad peak between 3000 cm^{-1} and 3300 cm^{-1} significantly decreased from 168 to 180 h because of the decomposition of PVA chain in chlorine solution as shown in Scheme 1a.

The gradually increase in water flux could be well explained by the increased surface hydrophilicity after immersing in the NaClO solution as shown in Fig. 7d where the water contact angles decreased from 77.8° to 73°. This should be caused by the formation of –COOH by

Table 3
Desalination performances before and after chlorine treatments.

Membrane ID	Before treatment		NaClO concentration (ppm. h)	After treatment	
	Flux	Rejection		Flux	Rejection
PVA-Ce (IV)/ PSF [22]	55.3	96	4000	66.4	93
PVA-GA/PA [21]	26.5	98.6	31200	41.2	95.5
PVA-DGEBA/ PF127 [49]	–	98	8000	–	95
NaAlg-PVA/PSF [50]	80	46	80000	85	40
PVA-FS/PVDF	33.0	99.9	336000	40.8	99.9

PF127: Pluronic F127; PA: polyamide. Flux: kg·m^{-2}·h^{-1}; Rejection: %.

chlorination. When the soaking time increased from 151 to 180 h, a rapid decrement in water contact angle was observed, indicating the formation rate of –COOH groups increased. This showed that the decomposition process of PVA was accelerated. Therefore, the integrity of the PVA-FS layer was destroyed after 180 h and led to the decrement in salt rejection. In addition, the zeta potentials slowly dropped from the −19.02 ± 0.1 mV to −22.3 mV in the first 151 h and then rapidly increased to −10.41 ± 0.69 mV. The decrease in surface charge was mainly due to the formation of negatively charged COO^{-} groups. After 180 h of chlorine treatment, the dense PVA-FS layer was damaged. The electrolyte could contact with the PVDF support which had neutral surface. Therefore, the surface electro-negativity increased. Table 3 compared the chlorine resistances among different membranes. The NaClO concentration was defined as the concentration of NaClO multiplied the soaking time in hour. It could be seen that the PVA-FS membrane exhibited an excellent chlorine resistance in harsh chlorine environment.

3.5. Acid and alkali resistances evaluation

PVA was crosslinked via the esterification reaction. The ester group would be hydrolyzed in both acid and base environments [51]. Sustainabilities of the PV composite membranes were evaluated by monitored the salt rejection of the membranes being soaked in acid or base solutions. As shown in Fig. 8, when soaked the membranes in both pH = 2 and pH = 12 solutions, salt rejections of the FS-3100, SPTA and P(AA-AMPS) crosslinked membranes could be maintained over 99.9% for 180 h, 80 h, and 100 h, respectively. The PVA-FS membranes showed the best chemical stability. When the pH value changed to 1 or 13, the salt rejections of the PVA-FS membranes could be maintained for 120 h. The excellent acid and base stability could be attributed to the intrinsic chemical stability of the fluorocarbon segments from the FS-3100 crosslinker.

3.6. Membrane fouling and washing tests

HA and Tween20 were chosen as typical protein and organic foulants. The fouling behavior and flux recovery of the PVA-FS/PVDF membranes were shown in Fig. 9. The stable pure water fluxes of two membranes were 44 ± 2 and 42 ± 1 kg m^{-2} h^{-1}, respectively. After

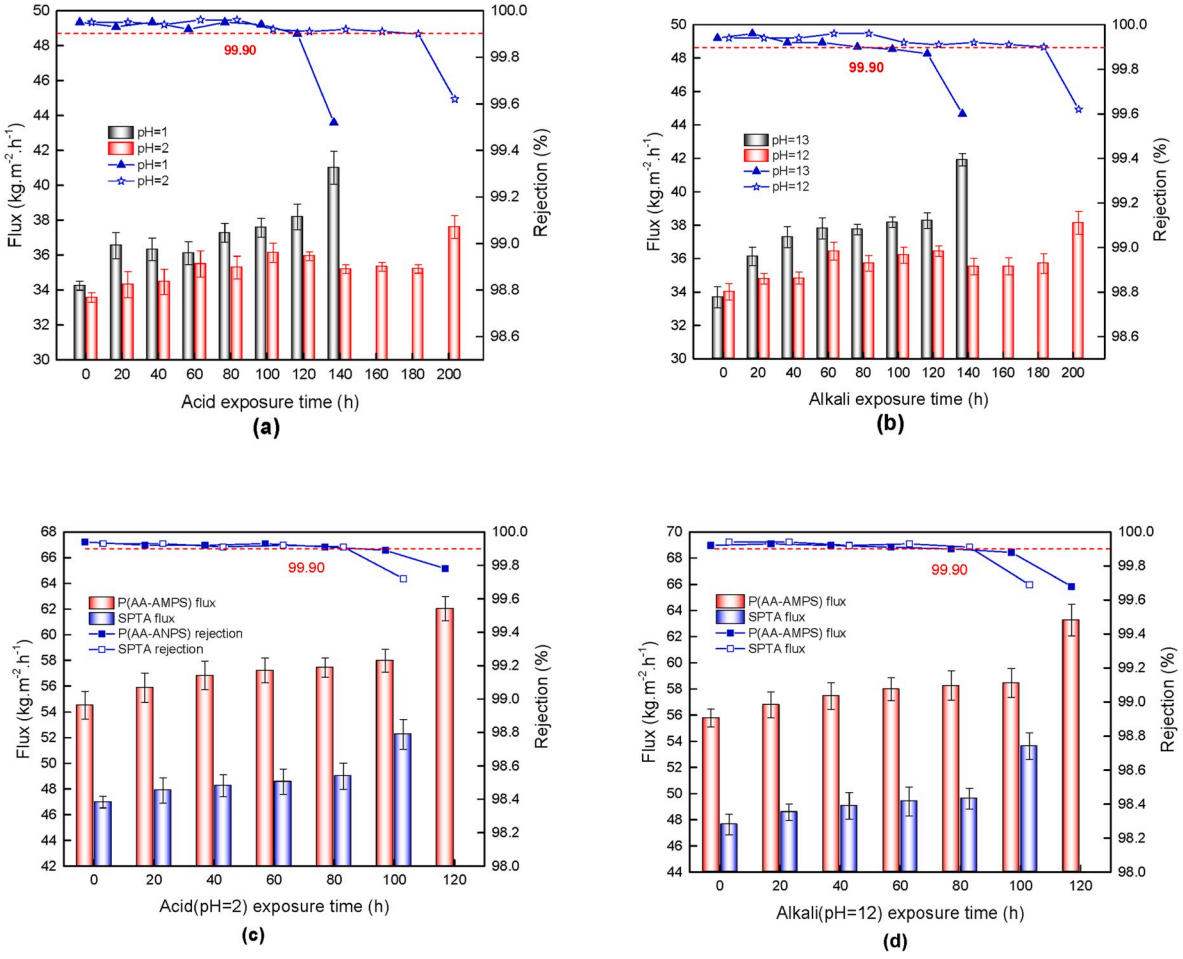

Fig. 8. Acid (a) and alkali (b) resistance property of PVA-FS membranes, (c) acid resistance of PVA-SPTA and PVA-P(AA-AMPS) membranes in HCl (pH = 2), (d) alkali resistance of PVA-SPTA and PVA-P(AA-AMPS) membranes in NaOH (pH = 12).

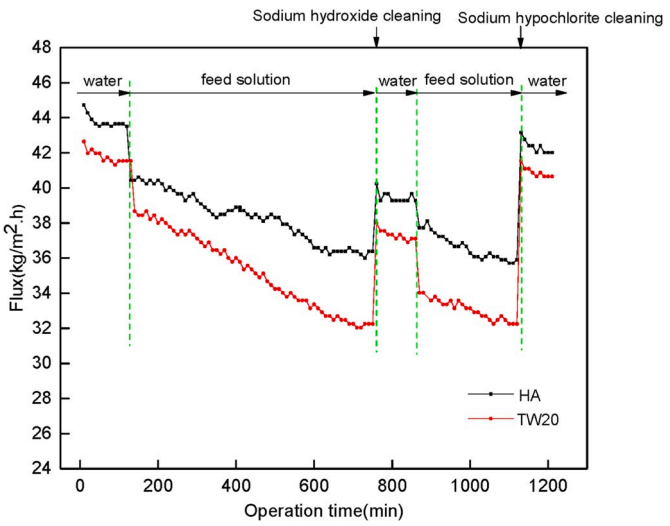

Fig. 9. Long-time operation measurement of the flux of the membranes with the filtration of model water solutions containing HA and Tween20. The fouled membranes were cleaned by NaOH(pH = 12) and 200 ppm NaClO (pH = 12).

adding HA and Tween20 into the feed solutions, a suddenly decreased water flux was observed where the water flux decreased from 44 ± 2 to 40 ± 1 kg m^{-2} h^{-1}, and 42 ± 1 to 38 ± 1 kg m^{-2} h^{-1}, respectively. This indicated that a fouling layer might be formed immediately. At the following 10 h, the fluxes of HA and Tween 20 solutions dropped to 36 ± 1 and 32 ± 1 kg m^{-2} h^{-1}, respectively. The gradually decreased fluxes resulted from more foulants absorbed on membrane surfaces. Note that, the fluorocarbon segments from FS-3100 increased surface hydrophobicity that led to a higher tendency to organic fouling. The fouling caused by Tween 20 was severer than by HA. This was because of the membrane surface absorbed with Tween 20 was more likely to adsorb micelles and build-up cake layer more quickly [52]. After washed by NaOH (pH = 12) solution for 30 min, the pure water flux returned to 40 ± 1 and 38 ± 1 kg m^{-2} h^{-1}, respectively. These fluxes were exactly the same to the starting water fluxes of the membranes after instantaneous fouling. This indicated that most of the organic fouling could be washed away by base solution except for the immediately formed fouling layers. In the next 5 h of fouling tests, water fluxes decreased to 36 ± 1 kg m^{-2} h^{-1} and 32 ± 1 kg m^{-2} h^{-1}, respectively. The more rapid decrements in water fluxes were due to that the instantaneous drops in water fluxes at the beginning of fouling tests. These phenomena were reported in membrane washing process for RO/UF membranes [53]. This was explained by the exposure of membrane surface after cleaning that was more easily adsorbed by foulants than the surface of cake layer. Notably, the membrane fluxes were approximately recovered to the initial fluxes of 44 ± 2 and 42 ± 1 kg m^{-2} h^{-1}, respectively, after being washed using the NaClO solution. This proved that ClO^- was more effective because HA would be oxidized into small molecules and Tween20 would be broke down into hydrophilic amides by hydrolysis. Since the PVA-FS (1:80) polymer were stable in NaClO solution (200 ppm) for 1680 h, the PV composite membrane would have a service life of 3.8 years if a chemical cleaning with 200 ppm NaClO was carried out for 0.5 h after 10 h of operation time.

4. Conclusions

We used a fluorine based crosslinker, FS-3100, to crosslink a modified PVA polymer where the 1, 2 diol units were removed to increase its chlorine resistance. The PVA-FS/PVDF composite membranes showed much better chemical resistances to acid, alkali, and chlorine solutions that were typical chemical compounds for membrane washing. The long term PV desalination experiments with periodic membrane washing treatments demonstrated that the membrane flux could be recovered to 100% after chemical cleaning.

Additional information

The authors declare no competing interests.

Declaration of competing interest

The authors declare no competing interests.

Acknowledgement

This research is funded by National Natural Science Foundation of China (51773011).

References

[1] Q. Li, B. Cao, P. Li, Fabrication of high performance pervaporation desalination composite membranes by optimizing the support layer structures, Ind. Eng. Chem. Res. 57 (2018) 11178–11185, https://doi.org/10.1021/acs.iecr.8b02505.
[2] Q. Wang, N. Li, B. Bolto, M. Hoang, Z. Xie, Desalination by pervaporation: a review, Desalination 387 (2016) 46–60, https://doi.org/10.1016/j.desal.2016.02.036.
[3] X.L. Cao, J.L. Guo, J. Cai, M.L. Liu, S.W.H. Xing, S.P. Sun, The encouraging improvement of polyamide nanofiltration membrane by cucurbituril-based host–guest chemistry, AIChE J. 66 (2020), e16879, https://doi.org/10.1002/aic.16879.
[4] M. Elimelech, W.A. Phillip, The future of seawater desalination: energy, Technology, and the environment, ence 333 (2011) 712–717, https://doi.org/10.1126/science.1200488, 6043.
[5] Y.L. Xue, C.H. Lau, B. Cao, P. Li, Elucidating the impact of polymer crosslinking and fixed carrier on enhanced water transport during desalination using pervaporation membranes, J. Membr. Sci. 575 (2019) 135–146, https://doi.org/10.1016/j.memsci.2019.01.012.
[6] Y.L. Xue, J. Huang, C.H. Lau, B. Cao, P. Li, Tailoring the molecular structure of crosslinked polymers for pervaporation desalination, Nat. Commun. 11 (2020) 1, https://doi.org/10.1038/s41467-020-15038-w.
[7] Q.F. An, F. Li, Y.L. Ji, H.L. Chen, Influence of polyvinyl alcohol on the surface morphology, separation and anti-fouling performance of the composite polyamide nanofiltration membranes, J. Membr. Sci. 367 (2011) 158–165, https://doi.org/10.1016/j.memsci.2010.10.060, 1-2.
[8] X.L. Ma, Y.L. Su, Q. Sun, Y.Q. Wang, Z.Y. Jiang, Enhancing the antifouling property of polyethersulfone ultrafiltration membranes through surface adsorption crosslinking of poly (vinyl alcohol), J. Membr. Sci. 300 (2007) 71–78, https://doi.org/10.1016/j.memsci.2007.05.008.
[9] H.G. Sun, Y.Q. Zhang, H. Sadam, J. Ma, Y.P. Bai, X. Shen, J.K. Kim, L. Shao, Novel mussel-inspired zwitterionic hydrophilic polymer to boost membrane water-treatment performance, J. Membr. Sci. 582 (2019) 1–8, https://doi.org/10.1016/j.memsci.2019.03.086.
[10] X.B. Yang, L.L. Yan, Y.D. Wu, Y.Y. Liu, L. Shao, Biomimetic hydrophilization engineering on membrane surface for highly-efficient water purification, J. Membr. Sci. 589 (2019) 117223, https://doi.org/10.1016/j.memsci.2019.117223.
[11] L. Li, J.W. Hou, Y. Ye, J. Mansouri, V. Chen, Composite PVA/PVDF pervaporation membrane for concentrated brine desalination: salt rejection, membrane fouling and defect control, Desalination 422 (2017) 49–58, https://doi.org/10.1016/j.desal.2017.08.011.
[12] E. Zondervan, B. Roffel, Evaluation of different cleaning agents used for cleaning ultra filtration membranes fouled by surface water, J. Membr. Sci. 304 (2007) 40–49, https://doi.org/10.1016/j.memsci.2007.06.041, 1–2.
[13] H.C. Kim, B.A. Dempsey, Membrane fouling due to alginate, SMP, EfOM, humic acid, and NOM, J. Membr. Sci. 428 (2013) 190–197, https://doi.org/10.1016/j.memsci.2012.11.004.
[14] W.S. Ang, S. Lee, M. Elimelech, Chemical and physical aspects of cleaning of organic-fouled reverse osmosis membranes, J. Membr. Sci. 272 (2006) 198–210, https://doi.org/10.1016/j.memsci.2005.07.035, 1–2.
[15] S.S. Madaeni, Y. Mansourpanah, Chemical cleaning of reverse osmosis membranes fouled by whey, Desalination 161 (2004) 13–24, https://doi.org/10.1016/S0011-9164(04)90036-7, 1.
[16] X. Shi, G. Tal, N.P. Hankins, V. Gitis, Fouling and cleaning of ultrafiltration membranes: a review, J. Water Process Eng. 1 (2014) 121–138, https://doi.org/10.1016/j.jwpe.2014.04.003.
[17] K.L. Cho, A.J. Hill, F. Caruso, S.E. Kentish, Chlorine resistant glutaraldehyde crosslinked polyelectrolyte multilayer membranes for desalination, Adv. Mater. 27 (2015) 17, https://doi.org/10.1002/adma.201570117, 2811-2811.
[18] L.L. Xia, C.L. Li, Y. Wang, In-situ crosslinked PVA/organosilica hybrid membranes for pervaporation separations, J. Membr. Sci. 498 (2016) 263–275, https://doi.org/10.1016/j.memsci.2015.10.025.
[19] R. Castromunoz, J. Bueragonzalez, O. de la Iglesia, F. Galiano, V. Fila, M. Malankowska, C. Rubio, A. Figoli, C. Tellez, J. Coronas, Towards the dehydration of ethanol using pervaporation cross-linked poly(vinyl alcohol)/

graphene oxide membranes, J. Membr. Sci. 582 (2019) 423–434, https://doi.org/10.1016/j.memsci.2019.03.076.
[20] R. Castromunoz, O. de la Iglesia, V. Fila, C. Tellez, J. Coronas, Pervaporation-assisted esterification reactions by means of mixed matrix membranes, Ind. Eng. Chem. Res. (2018), https://doi.org/10.1021/acs.iecr.8b01564 acs.iecr.8b01564-.
[21] M. Liu, Q. Chen, L. Wang, S. Yu, C. Gao, Improving fouling resistance and chlorine stability of aromatic polyamide thin-film composite RO membrane by surface grafting of polyvinyl alcohol (PVA), Desalination 367 (2015) 11–20, https://doi.org/10.1016/j.desal.2015.03.028.
[22] H.H. Rana, N.K. Saha, S.K. Jewrajka, A.V.R. Reddy, Low fouling and improved chlorine resistant thin film composite reverse osmosis membrane by cerium((IV)/polyvinyl alcohol mediated surface modification, Desalination 347 (2015) 93–103, https://doi.org/10.1016/j.desal.2014.11.013.
[23] N. Li, Z.Z. Lui, S.G. Xu, Dynamically formed poly (vinyl alcohol) ultrafiltration membranes with good anti-fouling characteristics, J. Membr. Sci. 169 (2000) 17–28, https://doi.org/10.1016/S0376-7388(99)00327-0, 1.
[24] W. Falath, A. Sabir, K.I. Jacob, Novel reverse osmosis membranes composed of modified PVA/Gum Arabic conjugates: biofouling mitigation and chlorine resistance enhancement, Carbohydr. Polym. 155 (2017) 28–39, https://doi.org/10.1016/j.carbpol.2016.08.058.
[25] G.C. Amine, S.D. Wadekar, H.U. Mehta, Kinetics and mechanism of hypochlorite oxidation of polyvinyl alcohol, Indian J. Textil. Res. 1 (1977) 20–23, 02, http://hdl.handle.net/123456789/33336.
[26] L.C. Hsu, D.W. Sheibley, Inexpensive cross-linked polymeric separators made from water-soluble polymers, J. Electrochem. Soc. 129 (1982) 251–254, https://doi.org/10.1149/1.2123807, 2.
[27] E. Broda, Geiger counting of carbon dioxide, J. Inorg. Nucl. Chem. 1 (1955) 411–412, https://doi.org/10.1016/0022-1902(55)80051-6, 6.
[28] K. Nakamae, T. Nishino, H. Ohkubo, S. Matsuzawa, K. Yamaura, Studies on the temperature dependence of the elastic modulus of crystalline regions of polymers: 14. Poly (vinyl alcohol) with different tacticities, Polymer 33 (1992) 2581–2586, https://doi.org/10.1016/0032-3861(92)91141-N, 12.
[29] P. Lu, S. Liang, T. Zhou, T. Xue, X. Mei, Q. Wang, Layered double hydroxide nanoparticle modified forward osmosis membranes via polydopamine immobilization with significantly enhanced chlorine and fouling resistance, Desalination 421 (2017) 99–109, https://doi.org/10.1016/j.desal.2017.04.030.
[30] S. Lin, H. Huang, Y. Zeng, L. Zhang, L.A. Hou, Facile surface modification by aldehydes to enhance chlorine resistance of polyamide thin film composite membranes, J. Membr. Sci. 518 (2016) 40–49, https://doi.org/10.1016/j.memsci.2016.06.032.
[31] K.S. Lee, M.H. Jeong, J.P. Lee, J.S. Lee, End-group cross-linked poly (arylene ether) for proton exchange membranes, Macromolecules 42 (2009) 584, https://doi.org/10.1021/ma802233j.
[32] S. Bonyadi, T.S. Chung, Highly porous and macrovoid-free PVDF hollow fiber membranes for membrane distillation by a solvent-dope solution co-extrusion approach, J. Membr. Sci. 331 (2009) 66, https://doi.org/10.1016/j.memsci.2009.01.014.
[33] H.C. Lee, H.S. Hong, Y.M. Kim, S.H. Choi, M.Z. Hong, H.S. Lee, K. Kim, Preparation and evaluation of sulfonated-fluorinated poly (arylene ether) membranes for a proton exchange membrane fuel cell (PEMFC), Electrochim. Acta 49 (2004) 2315–2323, https://doi.org/10.1016/j.electacta.2004.01.012, 14.
[34] S.M. Xue, C.H. Ji, J.L. Xu, Y.J. Tang, R.H. Li, Chlorine resistant TFN nanofiltration membrane incorporated with octadecylamine-grafted GO and fluorine-containing monomer, J. Membr. Sci. 545 (2018) 185–195, https://doi.org/10.1016/j.memsci.2017.09.075.
[35] Y. Li, B. Cao, P. Li, Effects of dope compositions on morphologies and separation performances of PMDA-ODA polyimide hollow fiber membranes in aqueous and organic solvent systems, Appl. Surf. Sci. 473 (2019) 1038–1048, https://doi.org/10.1016/J.APSUSC.2018.12.245.
[36] J.Q. Meng, C.H. Lau, Y.L. Xue, R. Zhang, B. Cao, P. Li, Compatibilizing hydrophilic and hydrophobic polymers via spray coating for desalination, J. Mater. Chem. 8 (2020) 8462–8468, https://doi.org/10.1039/D0TA00871K.
[37] K. Sugiura, M. Hashimoto, S. Matsuzawa, K. Yamaura, Influence of degree of crystallinity and syndiotacticity on infrared spectra of solid PVA, J. Appl. Polym. Sci. 82 (2001) 1291–1298, https://doi.org/10.1002/app.1963, 5.
[38] A. Vetere, Empirical method to correlate and to predict the Vapor−Liquid equilibrium and Liquid−Liquid equilibrium of binary amorpous polymer solutions, Ind. Eng. Chem. Res. 37 (1998) 2864–2872, https://doi.org/10.1021/ie9708891, 7.
[39] M.H.V. Mulder, C.A. Smolders, The mechanism of separation of ethanol/water mixture by pervaporation (I) calculation of concentration profiles, J. Membr. Sci. 17 (1984) 289, https://doi.org/10.1016/S0376-7388(00)83220-2.
[40] C.Y. Liang, F.G. Pearson, Approximate normal vibrations of crystalline polyvinyl alcohol, J. Polym. Sci. 35 (1959) 303–307, https://doi.org/10.1002/pol.1959.1203512836, 128.
[41] R.W. Baker, J.G. Wijmans, Y. Huang, Permeability, permeance and selectivity: a preferred way of reporting pervaporation performance data, J. Membr. Sci. 348 (2010) 346–352, https://doi.org/10.1016/j.memsci.2009.11.022, 1-2.
[42] R. Castromunoz, F. Galiano, O. de la Iglesia, V. Fila, C. Tellez, J. Coronas, A. Figoli, Graphene oxide–filled polyimide membranes in pervaporative separation of azeotropic methanol−MTBE mixtures, Separ. Purif. Technol. 224 (2019) 265–272, https://doi.org/10.1016/j.seppur.2019.05.034.
[43] W.F. Chan, E. Marand, S.M. Martin, Novel zwitterion functionalized carbon nanotube nanocomposite membranes for improved RO performance and surface anti-biofouling resistance, J. Membr. Sci. 509 (2016) 125–137, https://doi.org/10.1016/j.memsci.2016.02.014.
[44] M. Shi, Z. Wang, S. Zhao, J.X. Wang, S.C. Wang, A support surface pore structure re-construction method to enhance the flux of TFC RO membrane, J. Membr. Sci. 541 (2017) 39–52, https://doi.org/10.1016/j.memsci.2017.06.087.
[45] B. Liang, Q. Li, B. Cao, P. Li, Water permeance, permeability and desalination properties of the sulfonic acid functionalized composite pervaporation membranes, Desalination 433 (2018) 132–140, https://doi.org/10.1016/j.desal.2018.01.028.
[46] J.Q. Meng, P. Li, B. Cao, High-flux direct-contact pervaporation membranes for desalination, ACS Appl. Mater. Interfaces 11 (2019) 28461–28468, https://doi.org/10.1021/acsami.9b08078, 31.
[47] G. Liu, J. Shen, Q. Liu, J. Xiong, J. Yang, Ultrathin two-dimensional MXene membrane for pervaporation desalination, J. Membr. Sci. (2017), https://doi.org/10.1016/j.memsci.2017.11.065. S0376738817325450.
[48] R. Zhang, X.Y. Xu, B. Cao, P. Li, Fabrication of high-performance PVA/PAN composite pervaporation membranes crosslinked by PMDA for wastewater desalination, Petrol. Sci. 15 (1) (2018) 148–158, https://doi.org/10.1007/s12182-017-0204-z.
[49] W. Falath, A. Sabir, K.I. Jacob, Highly improved reverse osmosis performance of novel PVA/DGEBA cross-linked membranes by incorporation of Pluronic F-127 and MWCNTs for water desalination, Desalination 397 (2016) 53–66, https://doi.org/10.1016/j.desal.2016.06. 019.
[50] S. Bano, A. Mahmood, S.J. Kim, K.H. Lee, Chlorine resistant binary complexed NaAlg/PVA composite membrane for nanofiltration, Separ. Purif. Technol. 137 (2014) 21–27, https://doi.org/10.1016/j.seppur.2014.09.024.
[51] R.A. Assink, M.C. Celina, D.P. Lang, Chemical and physical changes in a hydrolyzed poly(ester urethane), Abstr. Pap. Am. Chem. Soc. 219 (1999) U482, https://doi.org/10.1002/1096-987X(20001130)21:15<1353::AID-JCC3>3.0.CO;2-G, 15.
[52] R. Naim, I. Levitsky, V. Gitis, Surfactant cleaning of UF membranes fouled by proteins, Separ. Purif. Technol. 94 (2012) 39–43, https://doi.org/10.1016/j.seppur. 2012.03.031.
[53] J. Xue, Z.W. Jiao, R. Bi, R.N. Zhang, X.D. You, F. Wang, L.J. Zhou, Y.L. Su, Z. Y. Jiang, Chlorine-resistant polyester thin film composite nanofiltration membranes prepared with β-cyclodextrin, J. Membr. Sci. 584 (2019) 282–289, https://doi.org/10.1016/j.memsci.2019.04.077.